



HAL
open science

Experimental investigation of 3D shock waves on nonlinear acoustical vortices

Thomas Brunet, Jean-Louis Thomas, Régis Marchiano, François Coulouvrat

► **To cite this version:**

Thomas Brunet, Jean-Louis Thomas, Régis Marchiano, François Coulouvrat. Experimental investigation of 3D shock waves on nonlinear acoustical vortices. *Physics Procedia*, 2010, *Physics Procedia*, 3 (1), pp.905-911. 10.1016/j.phpro.2010.01.116 . hal-01233834

HAL Id: hal-01233834

<https://hal.science/hal-01233834>

Submitted on 1 Dec 2015

HAL is a multi-disciplinary open access archive for the deposit and dissemination of scientific research documents, whether they are published or not. The documents may come from teaching and research institutions in France or abroad, or from public or private research centers.

L'archive ouverte pluridisciplinaire **HAL**, est destinée au dépôt et à la diffusion de documents scientifiques de niveau recherche, publiés ou non, émanant des établissements d'enseignement et de recherche français ou étrangers, des laboratoires publics ou privés.



Distributed under a Creative Commons Attribution - NonCommercial - NoDerivatives 4.0 International License



International Congress on Ultrasonics, Universidad de Santiago de Chile, January 2009

Experimental investigation of 3D shock waves on nonlinear acoustical vortices

Thomas Brunet^{a,b}, Jean-Louis Thomas^{a,*}, Régis Marchiano^b, François Coulouvrat^b

^a Institut des NanoSciences de Paris (UMR CNRS 7588), Université Pierre et Marie Curie, Paris, France

^b Institut Jean le Rond d'Alembert (UMR CNRS 7190), Université Pierre et Marie Curie, Paris, France

Abstract

We report experimental results about the 3D structure of shock waves on nonlinear acoustical vortices (AV). We will investigate classical shock waves (in the direction of propagation) and the azimuthal ones (in the transverse plane). At last, both quasi-monochromatic and transient regimes will be considered.

Keywords: Acoustical vortices; nonlinear acoustics; phase singularity; shock waves

1. Introduction

Since Nye and Berry [1] introduced the concept of phase singularity in wave theory, wave dislocations have been intensively studied in many fields of physics. Phase singularities can be classified into three categories: edge, screw or mixed type dislocations. They are important features of a wave field because they are both generic and structurally stable. Physically, this means, respectively, that they are naturally produced in a wave field, and that a weak perturbation of the field does not eliminate them. Thanks to these properties of structural stability and genericity, wave dislocations have many interesting properties.

The phase singularity of the screw type has been widely studied in a particular field of optics called *singular optics* [2]. This screw type dislocation, called optical vortex (OV), confers to the phase a helical shape winding up around a line (Z -axis) where the amplitude vanishes and the phase is not defined. Considering a transverse plane (X,Y), e.g. perpendicular to the beam axis (Z), the phase is defined everywhere except at a single point corresponding to the projection of the beam axis. In this plane, the number of 2π -iterations achieved by the phase on a close contour around that point is called the topological charge, denoted m . The sense of the winding gives the sign of the topological charge: by convention, it is positive if counterclockwise and negative clockwise [3]. At the

* Corresponding author. Tel.: +33 (0)1 44 27 42 75 ; fax: +33 (0)1 43 54 28 78.

E-mail address: Jean-Louis.Thomas@insp.jussieu.fr.

axial point, the amplitude of the wave field is null and forms a dark core because of destructive interferences. The fields at two points symmetric in relation to the centre of the beam are dephased by π .

By analogy with optics, in acoustics the screw type dislocation is called *acoustical vortex* (AV). For example, the amplitude and phase of AV are given on Fig.1 for two topological charges ($m = 1$ and $m = 2$). Hefner and Marston [4] demonstrated the possibility of generating single acoustical vortices of charge $m = 1$ and proposed to use them for underwater alignment thanks to the very narrow zero amplitude associated with them. Gspan et al. [5] showed that these structures could be produced by optoacoustic generation. Thomas and Marchiano [6] demonstrated that the pseudo-angular momentum and the pseudoenergy of an acoustical vortex are related to its topological charge. Moreover, this relation was extended to the case of weak nonlinear acoustics, for which the analysis provides a conservation law for the ratio of the topological charge to the harmonic order [6,7]. Recently, Marchiano *et al* [8] have developed a temporal analysis of the behaviour and the interaction of AV, and have numerically predicted the existence of an azimuthal shock wave which has been recently experimentally observed by Brunet *et al* [9].

2. Experimental results

2.1. Nonlinear acoustical vortices

As previously done [7]-[9], we use the linear inverse filter technique [10] to synthesize acoustical vortices. It is based on the knowledge of the medium of propagation between the acoustical sources and the points where the "target" field should be synthesized, namely the control points. Once the propagation operator has been experimentally recorded, an appropriate numerical treatment is applied to compute the signals that the transducers have to emit to synthesize the desired field at the control points. Here, we choose to use the Gauss-Laguerre (GL) beams as the "target" pattern in the control plane to synthesize AV. Indeed, these beams are known to carry screw dislocations [11]. They have a limited spatial extension and, consequently, are of finite energy. In addition, GL beams are exact solutions of the linear paraxial wave equation.

The experimental setup is made of a new spherically focused array of 127 piezoelectric transducers mounted on a spherical cap with a geometrical focal length of 450 mm immersed in water. The transducers are of hexagonal shape with a 60 mm² surface. They are distributed on a compact hexagonal pattern with a 100 mm aperture. The amplitude and the phase of each transducer can be driven independently thanks to electronic amplifiers. The central frequency of the transducers is $f_0 = 1$ MHz corresponding to a time period $T_0 = 1 \mu\text{s}$. In water at 20°C, the sound velocity is about $c_0 = 1500\text{m/s}$, so the corresponding wavelength is $\lambda = 1.5$ mm.

To measure the instantaneous amplitude of the nonlinear acoustic field, we use a very fast response membrane hydrophone with a geometric diameter of 80 mm and an active sensor diameter of 0.2 mm. The recorded signals are sampled at 250 MHz and averaged over 32 times to improve the signal-to-noise ratio. At a fixed distance of propagation ($Z = 500\text{mm}$), step by step motors achieve the displacement of the hydrophone in both transverse directions (X, Y). The field is sampled with 6561 points regularly set on a square grid of $15 \times 15 \text{ mm}^2 (= 10\lambda \times 10\lambda)$ with a spatial step of 0.5 mm ($= \lambda/3$). To see more details about the experimental setup, one can refer to the recent work done by Brunet *et al* [9].

The RMS amplitude and the phase patterns are given for two single vortices of topological charge $m = 1$ and $m = 2$, at the fundamental frequency f_0 on Fig.1. The spatial shape of the RMS amplitude reminds the one of a "doughnut", a characteristic feature of vortices, either acoustical or optical. At the center of the beam, the pressure is very low while it is maximum on the ring. Then, the pressure decreases progressively and tends to vanish. The phase increases linearly with the polar angle and turns around the centre of the beam for which the value of the phase is undefined as previously mentioned in the introduction. Note that the radial curvature of equiphase lines is due to a classical diffraction effect as already observed in acoustics [7].

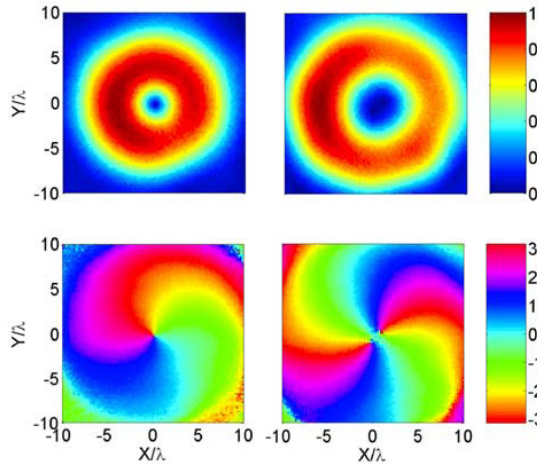


Fig.1 RMS amplitude (top view) and phase (bottom view) of the pressure field at the fundamental frequency in the plane (X,Y) for AV of charge +1 (left column) and +2 (right column).

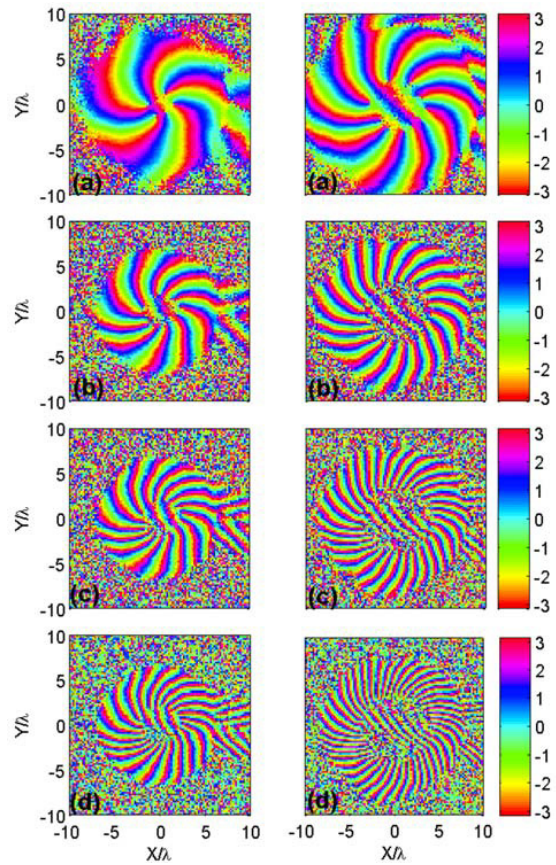


Fig.2 Phase for the (a) fifth, (b) tenth, (c) fifteenth and (d) twentieth harmonic of nonlinear AV ($m = 1$, left column) and ($m = 2$, right column) in the transverse plane (X,Y) .

For waves with finite amplitude, propagation is not linear: the speed of propagation depends on the instantaneous value of the pressure. Hence, the parts of the wave with high amplitude travel faster than those with low amplitude. As water is a quasi on-dispersive media for acoustic waves, it results into a distortion of the temporal profile. In terms of frequency spectrum, the counterpart of this nonlinear distortion is the generation of high order harmonics. Fig.2 shows the phase pattern measured on each point of the transverse plane (X,Y) for the fifth, tenth, fifteenth and twentieth harmonics for nonlinear AV of charge $m = 1$ (left column) and charge $m = 2$ (right column).

These figures allow us to access to the value of the topological charge for each harmonic frequency (respectively $m = 5, 10, 15, 20$ for an AV of charge +1, and $m = 10, 20, 30, 40$ for an AV of charge +2). Theoretically, the ratio between the total topological charge and the frequency has to be constant for propagation in an inviscid and isotropic medium [6]. Hence, the p^{th} harmonic of the fundamental will display a topological charge pq , if the charge of the fundamental is q . This law has already been checked in experiments for weak nonlinear effects (before the shock formation distance [6]) and extended to the case of parametric interaction between two AV [12]. Fig.2 shows that this law is here recovered, at least until the twentieth harmonics and so even for an AV of charge $m = 2$: its phase is made of $20 \times 2 = 40$ blades (Fig.2d). However, the limited spatial sampling of these measurements does not

allow us to observe higher harmonics. Indeed, the information contained by the phase becomes inaccessible as illustrated by the blurred zone which grows with harmonics order.

2.2. Temporal and azimuthal shock waves

It is well-known that nonlinear effects lead to the distortion of the temporal profile and finally to the formation of shock waves (Fig.3). This shock formation process is well-known for plane or focused waves but have recently been numerically predicted [8] and then observed experimentally [9] for AV.

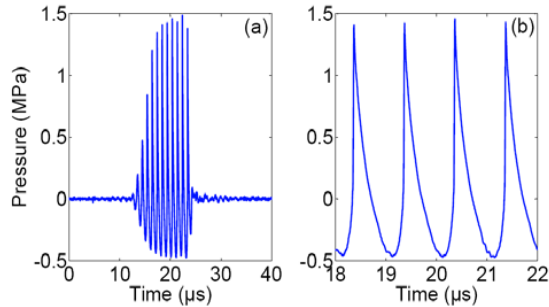


Fig.3 (a) Temporal signal of AV of charge $m = 1$. (b) Zoom on four cycles extracted from the middle of the wave train.

These observations show that the conservation law of the ratio between the frequency and the topological charge, mentioned in the last paragraph, remains valid beyond the shock formation distance. This result is far from obvious since the theoretical demonstration [6] was established for an isotropic and inviscid propagation medium. Here, the assumption of non dissipative medium is violated by the jump of entropy and the dissipation processes occurring through any shock. That result shows that the shocks do not destroy the stable structure of the AV and reinforces the concept of structural stability of AV with respect to nonlinear perturbations.

However, the main result of our work is about shock waves in the transverse plane, called *azimuthal shock waves*. Indeed, our measurements of the instantaneous pressure in the plane (X,Y) reveal sharp transitions in space, e.g. spatial shock waves, whose number corresponds to the topological charge m (Fig.4). In addition, the latter parameter sets their angular velocity as illustrated on Fig.4 showing the instantaneous pressure at five different times: t , $t+T_0/4$, $t+2T_0/4$, $t+3T_0/4$, $t+4T_0/4$. First, for $m = 1$, the single shock undergoes one revolution in one period T_0 exactly. Then, for $m = 2$, each of the two shocks propagates two times slower as illustrated by the black arrow on Fig.4.

To get a picture of the structure of these azimuthal shock waves, we show here 3D-reconstructions on Fig.5. With an appropriate algorithm, we are able to extract the position of the shock front in the transverse plane (X,Y) . Each time of measurement is assumed to correspond to a spatial position along the beam axis ($c_0 t = z$) allowing to unroll the AV structure in space along the beam axis. Thus, using shock waves as “markers”, one can visualize the helical wavefront whose step is equal to $m\lambda$. It is important to notice that this structure seems stable during the propagation: once the shock waves are formed, the shock front remains an helix.

In addition, the number of helices corresponds to the topological charge m . As shown on Fig.5, only one helix appears for $m = 1$ while two helices interlace for $m = 2$. In this latter case, for a same distance of propagation Z , the two simultaneously detected shocks correspond to two successive cycles.

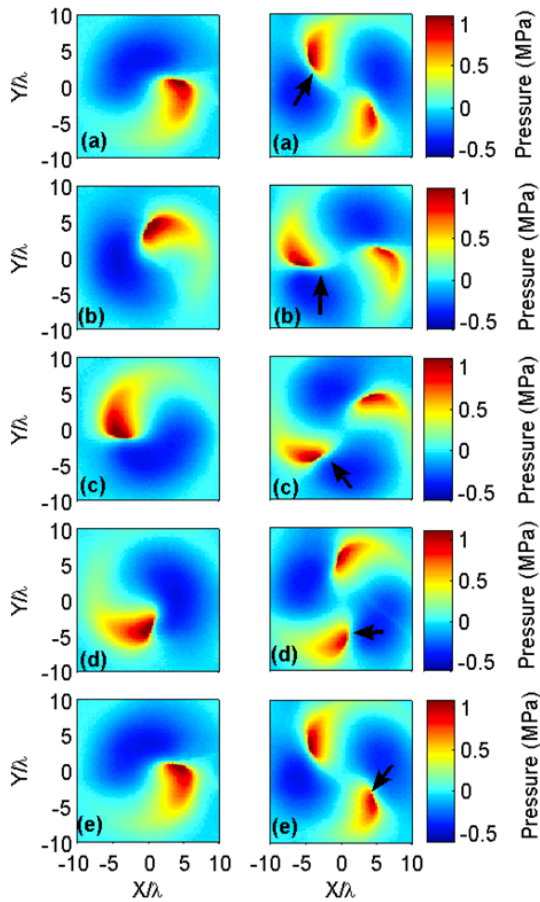


Fig.4 Instantaneous pressure of nonlinear AV for $m = 1$ (left column) and $m = 2$ (right column) in the plane (X,Y) at five different times (a) t , (b) $t+T_0/4$ (c) $t+2T_0/4$, (d) $t+3T_0/4$, (e) $t+T_0$. The black arrows are used to identify one specific shock.

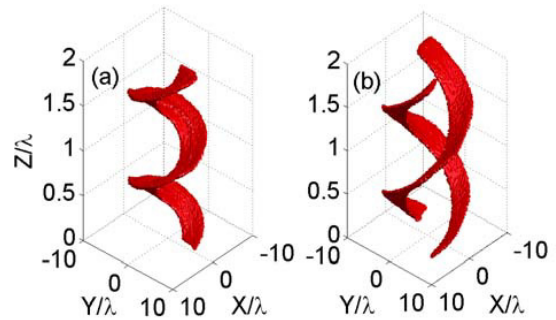


Fig.5 Shock front reconstruction from pressure measurements done in the transverse plane (X,Y) during two periods $2T_0$ for (a) $m = 1$ and (b) $m = 2$..

On Fig.6, we present the pressure amplitude for a duration Δt corresponding to one pitch of the helix. Here, the topological charge is 3 so $\Delta t = 3T_0 = 3\mu s$. On Fig.6a, the signal is quasi-monochromatic, three cycles and hence three shocks are visible. On Fig.6b, the signal is a pulse of about one cycle so only one shock is visible.

By reconstructing the front shock, one can recognize on Fig.7a three interlaced helices for the quasi-monochromatic regime corresponding to the three shocks visible on Fig.6a. As previously explained, their step is equal to $\Delta z = m\lambda$ so that here $\Delta z/\lambda = 3$. On the other hand, only one helix appears in the transient regime on Fig.7b as expected regarding to Fig.6b. This result demonstrates that the number of helices does not univocally depends on the topological charge m but also on the duration of the pulse. Hence, $1, 2, \dots, m$ shocks may be present depending on the number of cycles contained in the pulse.

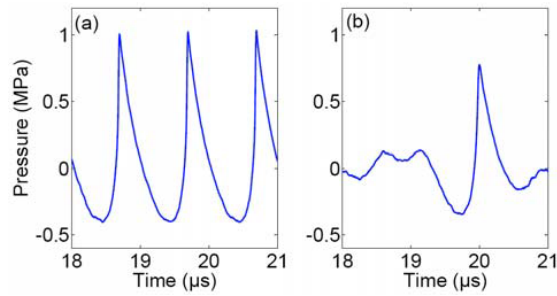


Fig.6 Temporal signal of AV for $m = 3$, for a duration $\Delta t = 3T_0$ (a) in quasi-monochromatic regime and (b) in transient regime

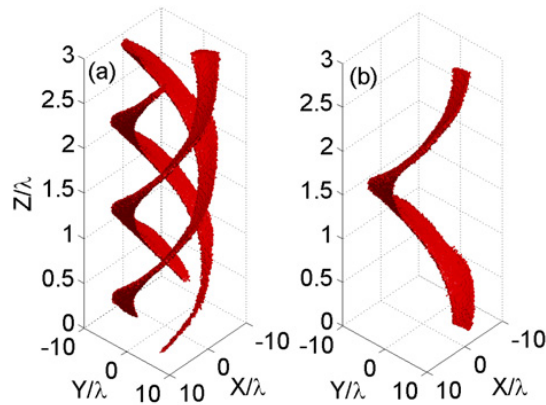


Fig.7 Shock front reconstruction from pressure measurements done in the transverse plane (X,Y) during three periods $3T_0$ for nonlinear AV of charge $m = 3$ (a) in quasi-monochromatic regime and (b) in transient regime.

3. Conclusion

The highlight of this paper is the experimental observation of azimuthal shock waves on nonlinear acoustical vortices for different topological charges ($m = 1$, $m = 2$ and $m = 3$). After recovering the conservation law between the topological charge and the harmonic order on fully developed shock waves, we investigated the helical structure of the shock waves. These experimental observations prove the stability of the acoustical vortices during propagation in both quasi-stationary and transient regimes.

These original results could be applied to design acoustical devices such as acoustical tweezers. In fact, acoustical spanners are very attractive because of their potential applications to manipulate small objects as recently suggested [13]-[14].

References

- [1] J. F. Nye and M. V. Berry, "Dislocations in wave trains," in Proc. R. Soc. Lond. A, vol. 336, pp. 165, 1974.
- [2] M. S. Soskin and M. V. Vassetsov, "Singular optics," in Prog. Opt., vol. 42, pp. 221, 2001.
- [3] M. Mansuripur and E. M. Wright, "in Opt. Photonics News," Opt. Photonics news, vol. 1, pp. 40, 1999.
- [4] B. T. Hefner and P. L. Marston, "An acoustical helicoidal wave transducer with applications for the alignment of ultrasonic and underwater systems," in J. Acoust. Soc. Am., vol. 106, pp. 3313, 1999.

- [5] S. Gspan, A. Meyer, S. Bernet and M. Ritsch-Marte, "Optoacoustic generation of a helicoidal ultrasonic beam," in *J. Acoust. Soc. Am.*, vol. 115, pp. 1142, 2004.
- [6] J.-L. Thomas and R. Marchiano, "Pseudo angular momentum and topological charge conservation for nonlinear acoustical vortices," in *Phys. Rev. Lett.*, vol. 91, pp. 244302, 2003.
- [7] R. Marchiano and J.-L. Thomas, "Synthesis and analysis of linear and nonlinear acoustical vortices," in *Phys. Rev. E*, vol. 71, pp. 066616, 2005.
- [8] R. Marchiano, F. Coulouvrat, L. Ganjehi and J.-L. Thomas, "Numerical investigation of the properties of nonlinear acoustical vortices through weakly heterogeneous media," in *Phys. Rev. E*, vol. 77, pp. 016605, 2008.
- [9] T. Brunet, J.-L. Thomas, R. Marchiano and F. Coulouvrat, "Experimental observation of azimuthal shock waves on nonlinear acoustical vortices," in *New. J. Phys.*, vol. 11, pp. 013002, 2009.
- [10] M. Tanter, J.-L. Thomas and M. Fink, "Time reversal and inverse filter," in *J. Acoust. Soc. Am.*, vol. 108, pp. 223, 2000.
- [11] R. Piestun, Y. Y. Schechner and J. Shamir, "Propagation-invariant wave fields with finite energy," in *J. Opt. Soc. Am.*, vol. 17, pp. 294, 2000.
- [12] R. Marchiano and J.-L. Thomas, "Doing arithmetic with nonlinear acoustical vortices," in *Phys. Rev. Lett.*, vol. 101, pp. 064301, 2008.
- [13] K. Volke-Sepúlveda, A.O. Santillan and R.R. Boulosa "Transfer of angular momentum to matter from acoustical vortices in free space," in *Phys. Rev. Lett.*, vol. 100, pp. 024302, 2008.
- [14] K.D. Skeldon, C. Wilson, M. Edgar and M.J. Padgett, "An acoustic spanner and its associated rotational Doppler shift," in *New. J. Phys.*, vol. 10, pp. 013018, 2008.